Published in final edited form as:
Sci Transl Med. 2014 March 12; 6(227): 227ra34. doi:10.1126/scitranslmed.3006927.

TGF-β signaling mediates endothelial to mesenchymal transition (EndMT) during vein graft remodeling

Brian C. Cooley[#1,*], **Jose Nevado**[#2,3], **Jason Mellad**[#4], **Dan Yang**[3], **Cynthia St. Hilaire**[3], **Alejandra Negro**[3], **Fang Fang**[3], **Guibin Chen**[3], **Hong San**[3], **Avram D. Walts**[3], **Robin L. Schwartzbeck**[3], **Brandi Taylor**[3], **Jan D. Lanzer**[3], **Andrew Wragg**[3,4], **Abdalla Elagha**[3,5], **Leilani E. Beltran**[3], **Colin Berry**[3,6], **Robert Feil**[7], **Renu Virmani**[8], **Elena Ladich**[8], **Jason C. Kovacic**[3,9], and **Manfred Boehm**[3]

[1] Department of Orthopaedic Surgery, Medical College of Wisconsin, Milwaukee, Wisconsin, 53226, USA.

[2] National Institutes of Health-University of the Philippines College of Medicine, Ermita, Manila.

[3]Center for Molecular Medicine, National Heart, Lung, and Blood Institute, National Institutes of Health, Bethesda, Maryland, 20892, USA.

[4]William Harvey Research Institute, Barts and the London NHS Trust, London, EC1M 6BQ, UK.

[5]Cardiovascular Department, Faculty of Medicine, Cairo University, Cairo 11559, Egypt.

[6]Institute of Cardiovascular and Medical Sciences, University of Glasgow, Glasgow G12 8TA, Scotland, UK.

[7]Interfaculty Institute of Biochemistry, Universität Tübingen, 72074 Tübingen, Germany.

[8]CVPath Institute, Inc., Gaithersburg, Maryland, 20878, USA.

[9]The Zena and Michael A. Wiener Cardiovascular Institute, Icahn School of Medicine at Mount Sinai, New York, NY, 10029, USA.

[#] These authors contributed equally to this work.

Abstract

Veins grafted into an arterial environment undergo a complex vascular remodeling process. Pathologic vascular remodeling often results in stenosed or occluded conduit grafts. Understanding this complex process is important for improving the outcome of patients with coronary and peripheral artery disease undergoing surgical revascularization. Using *in vivo* murine

Corresponding author: boehmm@nhlbi.nih.gov.
[*]Current affiliation: Dept. of Pathology and McAllister Heart Institute, University of North Carolina, Chapel Hill, North Carolina, 27599, USA

Author contributions: B.C.C. and H.S. performed surgeries; J.N., J.M., D.Y., C.S., A.N., F.F., G.C., A.W. and M.B. designed and/or performed immunostaining, western blotting, FACS, histological staining, and cell culture experiments; D.Y., C.S.H., and M. B. worked with human samples, J.N., D.Y., C.S., A.N., A.W., J.L. and M.B. analyzed data; MB provided funding; M.B., D.Y., C.S., A.N., J.K. wrote the paper; R.F. R.V. and E.L. provided specific reagents.

Competing interests: The authors declare no competing interests.

Data and materials availability: All murine models are available with MTA. Post-mortem human samples were obtained from CV Path Institute, Inc.

cell lineage-tracing models, we show that endothelial-derived cells contribute to neointimal formation through endothelial to mesenchymal transition (EndMT), which is dependent upon early activation of the Smad2/3-Slug signaling pathway. Antagonism of TGF-β signaling by TGF-β neutralizing antibody, shRNA-mediated Smad3 or Smad2 knockdown, Smad3 haploinsufficiency, or endothelial cell-specific Smad2 deletion resulted in decreased EndMT and less neointimal formation compared to controls. Histological examination of postmortem human vein graft tissue corroborated the changes observed in our mouse vein graft model, suggesting that EndMT is operative during human vein graft remodeling. These data establish that EndMT is an important mechanism underlying neointimal formation in interpositional vein grafts, and identifies the TGF-β/Smad2/3-Slug signaling pathway as a potential therapeutic target to prevent clinical vein graft restenosis.

Introduction

The treatment of coronary atherosclerosis is a major global health care expenditure. A substantial component of this expenditure is attributable to patients undergoing percutaneous coronary intervention or coronary artery bypass graft (CABG) surgery, with >160,000 CABG procedures performed annually in the United States alone (*1*). Veins are common conduits used in these surgical procedures however approximately 40% of vein grafts will fail within 12 – 18 months of implantation (*2*). This high failure rate is attributable to adverse vascular remodeling, yet the disease mechanisms regulating the pathophysiological changes involved remain poorly understood (*3*). Vascular remodeling is the result of the complex, dynamic interactions between various cell populations, including endothelial cells, mesenchymal smooth muscle-type cells, activated thrombocytes and infiltrating inflammatory cells (*4*-*6*). The cellular contributions to the remodeled vessels are generally considered to be lineage restricted (*7*), although the origin of the cells forming the neointima is highly controversial (*8*).

Endothelial-to-mesenchymal transition (EndMT) is the process by which endothelial cells lose their cell-specific markers and morphology and acquire a mesenchymal cell-like phenotype. EndMT is regulated by a complex orchestration of several signaling pathways (*9*) and has been implicated in chronic fibrosis (*10*) and in heterotopic ossification owing to fibrodysplasia ossificans progressiva (*11*). Recent studies indicate that EndMT may be involved in murine transplant arteriopathy (*12*), in the rejection of human transplant lesions (*12*), and in vascular cerebral cavernous malformations (*13*). However, the role of EndMT and the mechanisms regulating cell phenotype adaptation during human vein graft remodeling are poorly understood.

Here, we investigated EndMT during the neointimal hyperplasic response that occurs after grafting veins into the arterial circulation in both mice and humans. We demonstrated that endothelial lineage-derived cells comprise the majority of vascular neointimal cells formed during murine vein graft remodeling. Early failed human grafts also displayed features indicative of EndMT. Furthermore, we show that the TGF-β-Smad2/3-Slug signaling pathway plays a pivotal role in regulating vein graft EndMT, with *in vivo* reduction of TGF-β signaling decreasing both neointimal formation and the relative contribution of endothelial

lineage-derived cells to the neointima. These findings enhance our understanding of the molecular mechanisms underlying vascular remodeling and reveal novel targets for potential therapeutic interventions aimed at improving clinical outcomes following interpositional vein grafting.

RESULTS

Endothelial lineage–derived cells contribute to neointimal formation during vascular remodeling in mice

To examine the contribution of endothelial-derived cells to the neointima during vascular remodeling, interpositional vein grafting was performed using two independent endothelial lineage tracing systems; the constitutive *Endotrack*^{YFP} or *LacZ* (*14-16*) and the tamoxifen-inducible *Ind.Endotrack*^{YFP} transgenic mouse models (*17*). In these models, endothelial-specific *cre* gene expression irrevocably activates the reporter gene, resulting in continuous *YFP* or *LacZ* gene expression regardless of subsequent changes in cellular phenotype (*10, 14-19*). Prior to grafting, YFP expression within the jugular vein and perivascular region was observed in 98.5 ± 0.9% (SEM) of all *Endotrack*^{YFP} and 52.1 ± 6.1% (SEM) of all *Ind.Endotrack*^{YFP} endothelial cells (fig. S1A). YFP expression in native, ungrafted jugular veins was only observed in endothelial cells, which also stained positive for the endothelial cell marker CD31 (fig. S1A).

We grafted a branch of the jugular vein from the endothelial lineage-tracing mouse models into the femoral artery of genetically matched wild type recipients through end-to-end anastomosis (*20*). Graft placement with chronic exposure to arterial pressure induced a remodeling program, leading to neointimal formation. Endothelial-derived YFP-positive (YFP$^+$) cells were recruited to the neointima, representing 51.7 ± 3.3% and 27.8 ± 2.9% (SEM) of the total neointimal cell population at day 35 in the *Endotrack*^{YFP} and *Ind.Endotrack*^{YFP} veins, respectively (Fig. 1A). These findings were confirmed in long-term fate-tracking experiments, where endothelial-derived cells persisted and contributed to the neointima, at least until 90 days after transplantation (fig. S1B). No reporter gene activation was observed in non-recombined *Endotrack*^{YFP} or *Ind.Endotrack*^{YFP} grafted veins at day 35 (Fig. 1A). Similar results were obtained using veins isolated from the *Endotrack*^{LacZ} lineage-tracing model (fig. S1C).

Consistent with other mouse models of neointimal formation (*4, 5*), we found a progressive increase in the total number of neointimal cells between 3 and 14 days post-vein grafting (Fig. 1B). While the number of non-endothelial lineage (YFP$^-$) neointimal cells plateaued after 14 days, the number of neointimal YFP$^+$ cells continued to increase up to 35 days post-grafting (Fig. 1B). Similar to a prior report (*21*), we detected cell-cycle re-entry of YFP$^+$ cells (Fig. 1C and fig. S1, D and E).

There was a very low possibility that donor-derived YFP$^+$ hematopoietic cells contribute to vascular remodeling. Nevertheless, we analyzed ungrafted jugular veins prior to transplantation by FACS and did not detect any donor-derived hematopoietic stem cells or myeloid progenitor cells (fig. S2A). We also analyzed peripheral blood and bone marrow of recipient animals at 35 days post-grafting and did not detect any YFP$^+$ cells after vein

grafting (fig. S2, B to D). We did not identify any YFP^+ macrophages, T lymphocytes, or neutrophils within grafted vessels by immunohistochemistry (fig. S3, A to C), indicating that donor hematopoietic cells do not populate the vein graft or its neointima. We excluded possible non– endothelial-dependent Tie2 promoter activation using the transgenic *Tie2GFP* mouse line in which GFP is expressed transiently when the *Tie2* promoter is active (fig. S3D) (*22*). These experiments demonstrate that endothelial lineage–derived cells contribute to neointimal formation during vein graft remodeling.

Vein graft vascular remodeling involves EndMT

We addressed the phenotypic fate of the vein graft endothelium with respect to neointimal formation. Staining for three endothelial-specific markers (CD31, VE-cadherin, and endoglin) revealed that neointimal, but not luminal, YFP^+ cells progressively lost expression of these markers between 7 and 14 days after grafting (Fig. 2, A and B). With the exception of luminal cells, we did not detect expression of endothelial-specific markers on neointimal YFP^+ cells at day 35.

We examined YFP^+ cells for co-expression of early vascular smooth muscle cell (VSMC) markers, smooth muscle actin (SMA) and SM22α, the mature markers calponin, smoothelin, and VSMC-specific myosin heavy chain (SM-MHC). At day 0, no YFP^+ cells were detected that co-expressed any VSMC markers (Fig. 2, C to F). Thereafter, we observed a progressive increase in the number of YFP^+ cells that expressed the early VSMC markers SMA and SM22α (Fig. 2, C and D). By day 35, non-luminal neointimal YFP^+ cells lost the expression of all examined endothelial markers but uniformly expressed SMA and SM22α (Fig. 2, A to D). FACS analysis confirmed these histological findings: at day 0 a majority of YFP^+ cells were $CD31^+$ [83.2 ± 2.7% (SEM)], at day 35, nearly 85% of YFP^+ cells—representing the neointimal endothelial cell population—were SMA^+ whereas only 15% of these YFP^+ cells were $CD31^+$ (fig. S4, A and B). Less than 10% of YFP^+ cells expressed the more mature VSMC markers calponin or smoothelin (Fig. 2D). The fully differentiated VSMC marker, SM-MHC, was virtually undetectable in YFP^+ cells (Fig. 2E). By contrast, most YFP^- cells in the neointima expressed all five VSMC-specific markers (Fig. 2, E and F), consistent with these cells being of resident VSMC origin. At 7 days 93.9 ± 3.9% of cells co-staining for CD31 and SMA were YFP^+, indicating that these cells were of endothelial cell origin and in transition. At 7 days 16.0 ± 0.1% (SEM) of total neointimal cells were triple-positive for CD31, SMA, and YFP (Fig. 2G).

To further confirm that a proportion of neointimal cells were derived from endothelial cells, we used a smooth muscle cell–specific lineage-tracing model *Ind.SMCtrack^{YFP}* (*23*). The recombination efficiency of the *Ind.SMCtrack^{YFP}* system was 50.2% (YFP^+/$SM22α^+$ cells) or 51.1% (YFP^+/$SM\text{-}MHC^+$ cells) (fig. S5A). After vein grafting, we found that only 8.3% of all neointimal cells were YFP^+ (fig. S5B), which, based on the recombination efficiency of this mouse model, suggests that 16% of the neointimal cells were of VSMC origin.

Adventitial fibroblasts have also been attributed to neointimal formation during vascular remodeling (*24*); however, we were unable to detect a significant number of YFP^+ cells that co-expressed the fibroblast markers fibroblast-specific protein 1 (FSP-1) or fibroblast activation protein α (FAP) in the *Endotrack^{YFP}* grafted veins (fig. S6A). Only 10.4 ± 3.0%

(SEM) of neointimal cells co-expressed FSP-1 and SMA, representing the myofibroblast population and accounting for a minor population of neointimal cells (fig. S6B). The matrix markers fibronectin, tenascin, and collagen III, and the mesenchymal markers N-cadherin and Thy-1 were all expressed within the neointima at 35 days after grafting (fig. S7).

Activation of TGF-β signaling during vascular remodeling

TGF-β signaling in vascular remodeling is well documented (*25-27*), and has been implicated in EndMT during development and fibrotic remodeling (*18, 28*). In endothelial cells, TGF-β is known to mediate the sequential phosphorylation of ALK5 and Smad2/3, but its impact on ALK1 and Smad1/5/8 signaling remains controversial (*29, 30*). Murine jugular vein endothelial cells expressed TGFβRI/Alk5, TGFβRII, and ALK1 (fig. S8A). In grafted veins, phosphorylated Smad2/3 (p-Smad2/3) was detected in endothelial cells at days 3 and 7 post-grafting, which declined by day 14 and was undetectable by day 35 (Fig. 3A; fig. S8B). Individual p-Smad3 and p-Smad2 immunostaining showed similar activation as p-Smad2/3 (fig. S8C). In contrast, p-Smad1/5/8 was evident as early as 3 days after grafting but was present throughout the 35-day observation period in YFP^+ cells (Fig. 3A; fig. S8, C and D).

Next, we quantified the expression of established TGF-β–regulated transcription factors implicated in developmental EndMT: Slug, Twist, and Snail (*31*). Slug and Twist were activated predominantly in YFP^+ cells from 3-14 days after vein grafting, but were absent by day 35 (Fig. 3B; fig. S9, A and B). Conversely, in the early phase of remodeling (days 0–7) activation of Snail was barely detectable but was evident at day 35 post-grafting, where it was primarily restricted to YFP^- cells (fig. S9C). Immunoblotting using individual p-Smad and Slug antibodies corroborated the immunostaining data (Fig. 3C). The transient activation of Smad2/3 is consistent with the upregulation of Twist and Slug, and supports our hypothesis that TGF-β signaling triggers endothelial cell phenotypic fate changes during vein graft remodeling.

TGF-β–Smad2/3 signaling activates EndMT in murine endothelial cells

FACS analysis confirmed that TGFβRII, TGFβR1/Alk5, Alk1, and CD31 are expressed in murine endothelial hemangioendothelioma (mEOMA) cells and murine aortic endothelial cells (mAEC) (fig. S10A). Treatment of mEOMA cells and mAECs *in vitro* with TGF-β1 decreased the expression of the endothelial markers VE-cadherin and CD31, with a concurrent morphological change and upregulation of SM22α and F-actin (fig. S10B), indicative of *in vitro* EndMT. In mEOMA cells knockdown of Smad3 or Smad2 (fig. S11A) prevented TGF-β-induced EndMT (fig. S11B). Immunoblotting confirmed these immunostaining results (fig. S11C).

TGF-β—Smad2/3 signaling modulates EndMT during vein graft remodeling

The role of TGF-β in vein graft remodeling and the initiation of EndMT were investigated *in vivo*. Recipient mice were pre-treated with pan–TGF-β neutralizing antibody prior to grafting $Endotrack^{YFP}$ veins that were also treated by immersion in pan–TGF-β neutralizing antibody or control IgG *ex vivo* prior to grafting. Inhibition of TGF-β1 was verified by measuring plasma levels of total TGF-β1 (Fig. 4A) and by confirming diminished activation

of Smad2/3 at the 7-day time-point (fig. S12A). Consistent with our hypothesis, blocking TGF-β signaling inhibited EndMT by reducing neointimal area and YFP^+ cell contribution by day 35 compared to IgG-treated controls (Fig. 4, B to D). TGF-β inhibition did not substantially alter the extracellular matrix composition (fig. S12B).

TGF-β-Smad2/3-Slug signaling axis regulates EndMT during vein graft remodeling

We have shown thus far that TGF-β activates Smad2/3 and mediates EndMT both *in vitro* and *in vivo* in mice. We performed *in vivo* studies using *Endotrack*^{YFP} mouse veins incubated *ex vivo* with lentiviral shRNA targeting *Smad3* or *Smad2* prior to grafting. We observed a significant decrease in *Smad3* or *Smad2* mRNA after corresponding shRNA treatment (fig. S13A). Both Smad2 and Smad3 shRNA–treated grafts displayed significantly reduced YFP^+ cells and EndMT, and decreased neointimal formation at day 35 (Fig. 5).

We next tested whether the inhibition of Smad2 or Smad3 signaling in vein grafts altered the expression of Snail, Slug and Twist, as well as Smad-dependent activators of the mesenchymal program, myocardin and myocardin-related factors (MRF) a and b. These experiments revealed that *Smad3* knockdown significantly attenuated the expression of *Slug* and *MRFb* at the 3- and 7-day early time-points (fig. S13B). *Smad2* knockdown attenuated only the expression of *Slug*, whereas changes in *MRFb* expression did not reach statistical significance (fig. S13B). We used chromatin immunoprecipitation (ChIP) to demonstrate the direct binding of *Smad3* to the *Slug* promoter both *in vitro* (fig. S13C) and *in vivo* (fig. S13D), indicating that TGF-β–Smad2/3 signaling in vein graft remodeling transcriptionally regulates *Slug* directly.

We further investigated the role of Smad3 in EndMT during vein graft adaptation in a *Smad3* genetic knockout model, *Smad3;Endotrack*^{YFP} mice. Homozygous *Smad3* gene deletion results in severe growth deficiency and thus renders these mice unsuitable for vein graft experiments. Jugular veins from heterozygous *Smad3;Endotrack*^{YFP} mice were grafted into genetically matched wild type controls. At 35 days post-grafting, *Smad3* haploinsufficiency attenuated neointimal formation and EndMT (Fig. 6, A and B). Activation of Smad3, but not Smad1/5/8, was significantly decreased in these grafts (fig. S14). Lentiviral-mediated overexpression of *Slug* rescued the effect of *Smad3* haploinsufficiency on neointimal formation and EndMT after vein grafting (Fig. 6C). The role of endothelial Smad2 was examined in the *Smad2*$^{Fl/Fl}$*;Ind.Endotrack*^{YFP} line. Depletion of endothelial *Smad2* resulted in more favorable vascular remodeling and reduced EndMT (Fig. 6D). These findings are consistent with our Smad3 and Smad2 shRNA knockdown data (Fig. 4 and 5) and support the important role of Smad2/3 in TGF-β–dependent EndMT during vein graft remodeling.

EndMT in human endothelial cells and in human vein graft remodeling

We confirmed by FACS analysis that TGFβRII, TGFβR1/Alk5, and Alk1 are expressed in human umbilical vein endothelial cells (HUVECs) (fig. S15A). HUVECs treated with TGF-β1 showed increased expression of SM22α and Slug, and decreased expression of CD31 and VE-cadherin, compared with no treatment (Fig. 7A), which is indicative of EndMT. Similar to murine vein grafts, TGF-β1-treated HUVECs show increased gene expression of *Slug*,

Snail, and *Twist* (fig. S15B), suggesting that the TGF-β/Smad2/3-regulated transcriptional program is shared between species and plays a central role in orchestrating EndMT in human cells. Data from gene expression profiles comparing HUVECs, TGF-β1–treated HUVECs, and VSMCs show that TGF-β1-treatedHUVECs acquired a gene expression profile that was distinct from both untreated HUVECs and VSMCs (Fig. 7B). TGF-β1–treated HUVECs lost expression of markers expressed in the native HUVECs (e.g. CD31, vWF and endothelin 1) and gained expression of markers present in the primary VSMCs (e.g. αSMA, PDGF-β, LOX) indicative of EndMT in human cells.

To better understand the role of EndMT in human vein graft remodeling, we evaluated histological sections from newly acquired early-phase failed (<1 year, n=5) and long-term patent vein grafts (>6 year, n=5) stained with multiple endothelial cell markers [VE-cadherin, von Willebrand factor (vWF), and CD31] and immature (SMA and SM22α) or mature VSMC markers (SM-MHC and calponin). A subset of cells in the early vein graft neointimas co-stained for both endothelial and immature SMC markers, but not for mature VSMC markers (Fig. 7C, top panels), indicating that endothelial cells transition and acquire a VSMC-like phenotype during human vein graft remodeling. In the long-term patent grafts, only the luminal endothelial cells stained for endothelial cell markers and no double-positive cells were observed in the neointima (Fig. 7C, bottom panels). The human data corroborate our murine studies and underscores a role for EndMT in both human and mouse vein graft remodeling.

Discussion

Here we present evidence that EndMT is a central component of the vascular remodeling that occurs during vein adaptation to the arterial circulation in a murine model. At 35 days post-vein grafting half of the cells populating the neointima were of endothelial origin. These endothelial-derived cells lost their endothelial phenotype and acquired smooth muscle cell-like properties, yet failed to develop a fully ‘mature’ smooth muscle cell phenotype. We provide a mechanistic model demonstrating that TGF–β–Smad2/3–Slug signaling is a principal pathway regulating EndMT during vein graft remodeling. Importantly, examination of post-mortem human vein graft tissue confirmed that the process of EndMT is operative in human vein graft remodeling. Together these data identify new pathways regulating vascular remodeling that may be targeted for clinical interventions to improve outcomes following interpositional vein grafting in humans.

Supporting our *in vitro* findings, Medici *et al.* recently showed that TGF-β signaling promotes Snail-mediated EndMT via both Smad-dependent and -independent signaling (*32*), and studies using murine models have shown that endothelial cells participate in cardiac fibrosis via EndMT (*11, 18*). It is well known that during development TGF-β–mediated signaling contributes to emerging mesenchymal cell populations. Therefore, this study and others collectively support the hypothesis that TGF-β-mediated developmental programs are reactivated in response to injury or disease, and we propose that adult vein graft neointimal formation represents yet another biological setting where EndMT contributes to cardiovascular pathogenesis. Treatment strategies to attenuate TGF-β signaling in experimental cardiovascular disease models may include administration of a TGF-β

neutralizing antibody or a small molecule inhibitor to prevent vascular remodeling (*33*), as we have preliminarily demonstrated in mouse models to stop EndMT. The role of other TGF-β family members and downstream signaling pathways activated upon vein graft surgery and subsequent remodeling remains unclear. Specifically, neither the biological effects of BMP9/10–induced Smad1/5/8 signaling, nor the TGF-β-induced Smad1/5/8 activation was examined in this study. The role of BMP9/10– Smad1/5/8 in vein graft remodeling is currently unknown, and its relationship to Smad2/3 requires further investigation.

The use of genetically engineered mouse models enabled us to identify the cellular origins and molecular mechanisms contributing to the underlying pathology of vein graft remodeling, which is currently not possible with larger animal models or with humans. The cellular origins of the neointima during vascular remodeling have in part been attributed to differences in surgical technique (*34*). The vascular remodeling that occurs in end-to-end anastomoses differs from end-to-side anastomoses, in that the neointima in the former is comprised primarily of donor-derived cells, while the later recipient-derived (*35, 36*). Our study used end-to-end anastomoses to graft a branch of the jugular vein into the femoral artery. This technique resulted in substantial donor endothelial cell preservation, despite the increase in graft diameter and initial disruption of the venous endothelial layer due to increased arterial pressure. Although it may be argued that the combination of pressure-induced disruption of the endothelial cell layer with the preservation of select endothelial cell groups may facilitate EndMT, other dissimilarities between these vein graft models remain to be defined to account for the differing neointimal cellular contributions. Among the established murine vein graft models, our surgical model most closely replicates clinical vein-to-arterial grafting (*34*).

However, there are inherent differences between mouse and human anatomy and physiology, including differences in size, heart rate, and hemodynamic output, limiting the degree to which one can extrapolate these findings to human vein graft remodeling. For example, unlike human veins, mouse veins consist of a considerably thinner smooth muscle cell layer; the distending forces of acute-onset arterial pressure and flow might induce different degrees of vascular damage in comparison to human vein grafts. Further, due to size disparity, different surgical techniques are used to transplant mouse versus human veins, which may impact the remodeling process. Furthermore, endothelial cell lineage tracing studies are not feasible in humans; therefore, we examined post-mortem failed and long-term patent vein grafts. Corroborating our *in vitro* and murine studies, early-phase human vein grafts displayed molecular features that were strongly suggestive of EndMT.

In summary, our findings contribute to the greater understanding of the molecular mechanisms underlying human vascular remodeling and reveals novel targets against which potential therapeutic interventions can be developed for improving clinical outcomes following interpositional vein grafting. Toward translation, in a clinical study, treatment with the angiotensin-II receptor blocker Losartan significantly slowed the rate of pathologic aortic-root dilation in a small cohort of pediatric patients with Marfan syndrome (*37*). From the perspective of attenuating vein graft neointimal formation, given that TGF-β signaling is upregulated within hours after vein graft surgery (*38*), and that neointimal formation

plateaus and slows over the ensuing weeks and months, we speculate that the optimal window for clinical therapeutic intervention with anti–TGF-β therapies may be perioperative, and continued in the subsequent 2-6 weeks after graft surgery. Translation to the clinic will first require additional proof-of-concept studies in larger animal models to confirm the potential clinical benefit of modulating the TGF-β signaling pathway following vein graft surgery. These findings contribute to the greater understanding of the molecular mechanisms underlying human vascular remodeling, and reveals novel targets which may be translated into potential therapeutic interventions to improve clinical outcomes following interpositional vein grafting.

Materials And Methods

Study design

The study objective was to use *in vivo* endothelial cell lineage-tracing murine models to track and quantify donor vein endothelial cells grafted into the arterial circulation, characterize the molecular mechanisms regulating EndMT, and identify potential therapeutic targets. For all surgeries, numerical identifiers linking genotype/treatment of the donor sample were blinded to the scientist assessing/quantifying the results (e.g. counting co-stained cells). All experiments were replicated as indicated. The 3, 7, 14, and 35-day time points were selected based on (*20*), and our preliminary studies showed that there is no additional neointimal formation after the 35 day time point. A minimum of 4 patent mouse vein grafts were used in data analysis. Postmortem human samples were selected based on available samples that most closely approximated the mouse time points. Anonymized unstained sections of paraffin embedded human saphenous vein grafts were available from the CVPath Institute Sudden Death registry (CVPI-SCDRr) from hearts submitted in consultation (*39*).

Generation of animals

The National Heart, Lung and Blood Institute Animal Care and Use Committee approved all animal experiments. Primers used for genotyping are listed in table S1. *Endotrack*^{YFP}and *Endotrack*^{LacZ} mice were created by crossing the *Tie2Cre* (Jackson Laboratories) and *R26RstopYFP* and *R26RstopLacZ* lines, respectively (F. Constantini, Columbia University) (*14– 16*). The *Ind.Endotrack*^{YFP} line was created by breeding tamoxifen-inducble end*SclCreER*^{T} (C-M Hao, Vanderbilt University) (*17*) and *R26RstopYFP* lines. The *indSM22aCre*^{T} line was created by crossing *SM-CreERT2 (ki)* (R. Feil, University Tübingen, Germany) (*23*) and *R26RstopYFP* lines. The *Smad3;Endotrack*^{YFP} line was created by crossing heterozygous 129-Smad3<tm1Par>/J (Jackson Laboratories) and *Endotrack*^{YFP} lines. *Smad2*$^{Fl/Fl}$*;Ind.Endotrack*^{YFP} was created by crossing the *Smad2*$^{Fl/Fl}$ (M. Weinstein, Ohio State University) (*40*) and *Ind.Endotrack*^{YFP} lines. C57Bl/6J, 129S2/SvPasCrl and transgenic *(Tie2GFP)287Sato* (*22*) mice were purchased from Jackson Laboratories.

Induction of *cre* gene was achieved in four-week old mice by intraperitoneal injection of 1 mg of tamoxifen dissolved in 100 ul sterile peanut oil once daily for one week, followed by one week off, then a second course of injections daily for one week.

Vein grafting

Vein graft surgeries were performed as described in (*20*) where a vein graft was interpositioned via end-to-end anatomoses, detailed in Supplementary Methods.

Immunostaining

For immunostaining on fresh frozen tissues, thawed slides were washed in PBS and blocked using 5% donkey serum in PBS with 0.1% Triton-X100. For staining on formalin-fixed, paraffin-embedded human samples, slides were deparaffinized and underwent antigen retrieval. After blocking, primary antibodies were applied in 3% BSA overnight at 4°C, followed by the corresponding secondary antibody for one hour at RT and nuclei were stained with DAPI. Control slides were routinely stained in parallel by substituting IgG, or the specific IgG isotype. Protocol for BruD immunolabeling is outlined in detail in Supplementary Methods. All images were acquired using either a Zeiss Axioscope with AxioVision V4.3 software, a Zeiss LSM 510 UV laser scanning confocal microscope (Carl Zeiss, GmBH) or Nikon Eclipse TE300 inverted fluorescence microscope. Primary antibodies are outlined in table S2 and staining details outlined in Supplementary Methods.

Counting of co-stained cells

Slides were scanned using a confocal microscope, as described, at the stated magnification. Images were analyzed in a blinded manner. Specimen areas were divided into numbered grids and every cell pertaining to the neointimal region within the grid was counted. Total cell number within each grid was assessed by DAPI staining. Antibody-specific staining was assessed using filters specific for the corresponding secondary antibody fluorophore. YFP^+ cells were counted from images manually and expressed as the number of YFP^+ cells relative to total neointimal cells.

Morphology of neointima and cell counting

For morphological analysis of neointimal area, we first determined the ideal luminal area by calculating the area within the perimeter of the internal elastic lamina. Next, we measured the luminal area within the neointima (residual lumen). The difference between these values represents the neointimal area.

Cell lines and culture conditions

HUVECs (Lonza) and mEOMA cells (ATCC) were maintained according to manufacturer's instructions, detailed in Supplementary Methods.

Small hairpin RNA transfection

shRNA constructs for *Smad3*, *Smad2* and scrambled controls were purchased from Open Biosystems and prepared according to manufacturer's protocol and used as described in Supplementary Methods.

Neutralizing anti-TGF-β antibody treatment

Recipient mice were injected intraperitoneally with 10 mg/kg neutralizing anti-panTGF-β (Sigma) or control IgG one day prior to surgery, and every two weeks thereafter. Donor

veins were pretreated with 1 μg/ml neutralizing antibody or control IgG for 4 h at RT. Total TGF-β1 from plasma at specified timepoints was measured by ELISA according to the manufacturer's instructions (R&D Systems).

RNA extraction, reverse transcription, and real-time PCR

RNA was isolated from cultured cells using the RNeasy kit (Qiagen) according to the manufacturer's instructions. Details regarding extraction from tissue samples are outlined in Supplementary Methods. Primers are listed in table S1.

Western blot

Samples were lysed in RIPA buffer containing protease and phosphatase inhibitors (Sigma). For each sample, 20 μg of total protein was analyzed by Western blot (Biorad 4–20% Mini-PROTEAN TGX gel) and transferred onto nitrocellulose membranes. Antibodies used are listed on table S2.

Fluorescence-activated cell sorting (FACS)

Jugular veins and vein grafts were digested with 0.13 U/ml Liberase TM (Roche Apply Science) at 37°C for 20-25 min and digestion stopped with 20% FBS. Bone marrow and peripheral blood cells were incubated in Gey's solution and stained in FACS buffer, as detailed in Supplementary Methods.

Statistical Analyses

For cell culture, each experiment was repeated at least three times. Data are means ± SEM. After testing the normality of data by Shapiro-Wilks test, we applied the Student's t test for two conditions comparison or the one-way ANOVA test for time course comparison. If the condition levels are more than two, the Newman-Keuls Multiple Comparison correction was performed after ANOVA. Differences were deemed significant when $P < 0.05$. Statistical analyses were performed using Prism, Version 4.00 (GraphPad Software) and verified by Y. Yang (NHLBI).

Supplementary Material

Refer to Web version on PubMed Central for supplementary material.

Acknowledgments

We thank F. Constantini (Columbia University) for kindly providing *R26RstopYFP* & *R26RstopLacZ* mice, C.-M. Hao (Vanderbilt University) for the tamoxifen inducible end*SCLCreER*^{T} mice, and M. Weinstein (Ohio State University) for *Smad2*$^{Fl/Fl}$ mice. We thank the staff of the Laboratory of Animal Medicine and Surgery facility and L. McKennett for assistance with the transgenic mice. We acknowledge the professional skills and advice of C. A. Combs and D. Malide of the National Heart, Lung, and Blood Institute (NHLBI) Light Microscopy Core Facility, Z-X. Yu and colleagues at the NHLBI Pathology Core Facility, and statistical advice was provided by Y. Yang of the NHLBI DNA Sequencing and Computational Biology Core. **Funding:** This project was funded by the Intramural Research Program of the NHLBI. J. N. was supported by the Commission on Higher Education, the Philippine Council on Advanced Science and Technology Research, and Development Department of Science and Technology (PCASTRD-DOST) in the Philippines. J.M. was supported by an NIH Marshall Scholarship. J.K. is supported by NIH Grant K08HL111330. J.D.L. was supported by a Boehringer Ingelheim Fonds MD fellowship.

REFERENCES AND NOTES

1. Roger VL, Go AS, Lloyd-Jones DM, Adams RJ, Berry JD, Brown TM, Carnethon MR, Dai S, de Simone G, Ford ES, Fox CS, Fullerton HJ, Gillespie C, Greenlund KJ, Hailpern SM, Heit JA, Ho PM, Howard VJ, Kissela BM, Kittner SJ, Lackland DT, Lichtman JH, Lisabeth LD, Makuc DM, Marcus GM, Marelli A, Matchar DB, McDermott MM, Meigs JB, Moy CS, Mozaffarian D, Mussolino ME, Nichol G, Paynter NP, Rosamond WD, Sorlie PD, Stafford RS, Turan TN, Turner MB, Wong ND, Wylie-Rosett J. Heart disease and stroke statistics--2011 update: a report from the American Heart Association. Circulation. Feb 1.2011 123:e18. [PubMed: 21160056]
2. Mehta RH, Ferguson TB, Lopes RD, Hafley GE, Mack MJ, Kouchoukos NT, Gibson CM, Harrington RA, Califf RM, Peterson ED, Alexander JH. Saphenous Vein Grafts With Multiple Versus Single Distal Targets in Patients Undergoing Coronary Artery Bypass Surgery: One-Year Graft Failure and Five-Year Outcomes From the Project of Ex-Vivo Vein Graft Engineering via Transfection (PREVENT) IV Trial. Circulation. Jul 19.2011 124:280. [PubMed: 21709060]
3. Mitra AK, Gangahar DM, Agrawal DK. Cellular, molecular and immunological mechanisms in the pathophysiology of vein graft intimal hyperplasia. Immunol Cell Biol. Apr.2006 84:115. [PubMed: 16519729]
4. Boehm M, Olive M, True AL, Crook MF, San H, Qu X, Nabel EG. Bone marrow-derived immune cells regulate vascular disease through a p27(Kip1)-dependent mechanism. J Clin Invest. Aug.2004 114:419. [PubMed: 15286808]
5. Olive M, Mellad JA, Beltran LE, Ma M, Cimato T, Noguchi AC, San H, Childs R, Kovacic JC, Boehm M. p21Cip1 modulates arterial wound repair through the stromal cell-derived factor-1/CXCR4 axis in mice. J Clin Invest. Jun.2008 118:2050. [PubMed: 18464929]
6. Kovacic JC, Gupta R, Lee AC, Ma M, Fang F, Tolbert CN, Walts AD, Beltran LE, San H, Chen G, St Hilaire C, Boehm M. Stat3-dependent acute Rantes production in vascular smooth muscle cells modulates inflammation following arterial injury in mice. J Clin Invest. Jan 4.2010 120:303. [PubMed: 20038813]
7. Bentzon JF, Weile C, Sondergaard CS, Hindkjaer J, Kassem M, Falk E. Smooth muscle cells in atherosclerosis originate from the local vessel wall and not circulating progenitor cells in ApoE knockout mice. Arteriosclerosis, thrombosis, and vascular biology. Dec.2006 26:2696.
8. Nguyen AT, Gomez D, Bell RD, Campbell JH, Clowes AW, Gabbiani G, Giachelli CM, Parmacek MS, Raines EW, Rusch NJ, Speer MY, Sturek M, Thyberg J, Towler DA, Weiser-Evans MC, Yan C, Miano JM, Owens GK. Smooth muscle cell plasticity: fact or fiction? Circulation research. Jan 4.2013 112:17. [PubMed: 23093573]
9. Kovacic JC, Mercader N, Torres M, Boehm M, Fuster V. Epithelial-to-mesenchymal and endothelial-to-mesenchymal transition: from cardiovascular development to disease. Circulation. Apr 10.2012 125:1795. [PubMed: 22492947]
10. Zeisberg M, Yang C, Martino M, Duncan MB, Rieder F, Tanjore H, Kalluri R. Fibroblasts derive from hepatocytes in liver fibrosis via epithelial to mesenchymal transition. J Biol Chem. Aug 10.2007 282:23337. [PubMed: 17562716]
11. Medici D, Shore EM, Lounev VY, Kaplan FS, Kalluri R, Olsen BR. Conversion of vascular endothelial cells into multipotent stem-like cells. Nat Med. Nov 21.2010 16:1400. [PubMed: 21102460]
12. Chen PY, Qin L, Barnes C, Charisse K, Yi T, Zhang X, Ali R, Medina PP, Yu J, Slack FJ, Anderson DG, Kotelianski V, Wang F, Tellides G, Simons M. FGF regulates TGF-beta signaling and endothelial-to-mesenchymal transition via control of let-7 miRNA expression. Cell reports. Dec 27.2012 2:1684. [PubMed: 23200853]
13. Maddaluno L, Rudini N, Cuttano R, Bravi L, Giampietro C, Corada M, Ferrarini L, Orsenigo F, Papa E, Boulday G, Tournier-Lasserve E, Chapon F, Richichi C, Retta SF, Lampugnani MG, Dejana E. EndMT contributes to the onset and progression of cerebral cavernous malformations. Nature. Jun 27.2013 498:492. [PubMed: 23748444]
14. Kisanuki YY, Hammer RE, Miyazaki J, Williams SC, Richardson JA, Yanagisawa M. Tie2-Cre transgenic mice: a new model for endothelial cell-lineage analysis in vivo. Dev Biol. Feb 15.2001 230:230. [PubMed: 11161575]

15. Soriano P. Generalized lacZ expression with the ROSA26 Cre reporter strain. Nat Genet. Jan.1999 21:70. [PubMed: 9916792]
16. Srinivas S, Watanabe T, Lin CS, William CM, Tanabe Y, Jessell TM, Costantini F. Cre reporter strains produced by targeted insertion of EYFP and ECFP into the ROSA26 locus. BMC Dev Biol. 2001; 1:4. [PubMed: 11299042]
17. Göthert JR, Gustin SE, Hall MA, Green AR, Gottgens B, Izon DJ, Begley CG. In vivo fate-tracing studies using the Scl stem cell enhancer: embryonic hematopoietic stem cells significantly contribute to adult hematopoiesis. Blood. Apr 1.2005 105:2724. [PubMed: 15598809]
18. Zeisberg EM, Tarnavski O, Zeisberg M, Dorfman AL, McMullen JR, Gustafsson E, Chandraker A, Yuan X, Pu WT, Roberts AB, Neilson EG, Sayegh MH, Izumo S, Kalluri R. Endothelial-to-mesenchymal transition contributes to cardiac fibrosis. Nat Med. Aug.2007 13:952. [PubMed: 17660828]
19. Zeisberg EM, Potenta SE, Sugimoto H, Zeisberg M, Kalluri R. Fibroblasts in kidney fibrosis emerge via endothelial-to-mesenchymal transition. J Am Soc Nephrol. Dec.2008 19:2282. [PubMed: 18987304]
20. Cooley BC. Murine model of neointimal formation and stenosis in vein grafts. Arteriosclerosis, thrombosis, and vascular biology. Jul.2004 24:1180.
21. Ehsan A, Mann MJ, Dell'Acqua G, Tamura K, Braun-Dullaeus R, Dzau VJ. Endothelial healing in vein grafts: proliferative burst unimpaired by genetic therapy of neointimal disease. Circulation. Apr 9.2002 105:1686. [PubMed: 11940548]
22. Ohtsuki S, Kamiya N, Hori S, Terasaki T. Vascular endothelium-selective gene induction by Tie2 promoter/enhancer in the brain and retina of a transgenic rat. Pharm Res. Jun.2005 22:852. [PubMed: 15948028]
23. Kühbandner S, Brummer S, Metzger D, Chambon P, Hofmann F, Feil R. Temporally controlled somatic mutagenesis in smooth muscle. Genesis. Sep.2000 28:15. [PubMed: 11020712]
24. Holifield B, Helgason T, Jemelka S, Taylor A, Navran S, Allen J, Seidel C. Differentiated vascular myocytes: are they involved in neointimal formation? J Clin Invest. Feb 1.1996 97:814. [PubMed: 8609239]
25. Huang JS, Wang YH, Ling TY, Chuang SS, Johnson FE, Huang SS. Synthetic TGF-beta antagonist accelerates wound healing and reduces scarring. Faseb Journal. Aug.2002 16:1269. [PubMed: 12153996]
26. Jiang Z, Yu P, Tao M, Fernandez C, Ifantides C, Moloye O, Schultz GS, Ozaki CK, Berceli SA. TGF-beta- and CTGF-mediated fibroblast recruitment influences early outward vein graft remodeling. Am J Physiol Heart Circ Physiol. Jul.2007 293:H482. [PubMed: 17369455]
27. Jiang Z, Tao M, Omalley KA, Wang D, Ozaki CK, Berceli SA. Established neointimal hyperplasia in vein grafts expands via TGF-beta-mediated progressive fibrosis. Am J Physiol Heart Circ Physiol. Oct.2009 297:H1200. [PubMed: 19617405]
28. Zeisberg M, Hanai J, Sugimoto H, Mammoto T, Charytan D, Strutz F, Kalluri R. BMP-7 counteracts TGF-beta1-induced epithelial-to-mesenchymal transition and reverses chronic renal injury. Nat Med. Jul.2003 9:964. [PubMed: 12808448]
29. Goumans MJ, Liu Z, ten Dijke P. TGF-beta signaling in vascular biology and dysfunction. Cell Res. Jan.2009 19:116. [PubMed: 19114994]
30. Shi Y, Massague J. Mechanisms of TGF-beta signaling from cell membrane to the nucleus. Cell. Jun 13.2003 113:685. [PubMed: 12809600]
31. Hirasawa M, Noda K, Noda S, Suzuki M, Ozawa Y, Shinoda K, Inoue M, Ogawa Y, Tsubota K, Ishida S. Transcriptional factors associated with epithelial-mesenchymal transition in choroidal neovascularization. Molecular vision. 2011; 17:1222. [PubMed: 21617757]
32. Medici D, Potenta S, Kalluri R. Transforming growth factor-beta2 promotes Snail-mediated endothelial-mesenchymal transition through convergence of Smad-dependent and Smad-independent signalling. The Biochemical journal. Aug 1.2011 437:515. [PubMed: 21585337]
33. Habashi JP, Judge DP, Holm TM, Cohn RD, Loeys BL, Cooper TK, Myers L, Klein EC, Liu G, Calvi C, Podowski M, Neptune ER, Halushka MK, Bedja D, Gabrielson K, Rifkin DB, Carta L, Ramirez F, Huso DL, Dietz HC. Losartan, an AT1 antagonist, prevents aortic aneurysm in a mouse model of Marfan syndrome. Science. Apr 7.2006 312:117. [PubMed: 16601194]

34. Yu P, Nguyen BT, Tao M, Campagna C, Ozaki CK. Rationale and practical techniques for mouse models of early vein graft adaptations. J Vasc Surg. Aug.2010 52:444. [PubMed: 20573477]
35. Hu Y, Mayr M, Metzler B, Erdel M, Davison F, Xu Q. Both donor and recipient origins of smooth muscle cells in vein graft atherosclerotic lesions. Circulation research. Oct 4.2002 91:e13. [PubMed: 12364395]
36. Zhang L, Freedman NJ, Brian L, Peppel K. Graft-extrinsic cells predominate in vein graft arterialization. Arteriosclerosis, thrombosis, and vascular biology. Mar.2004 24:470.
37. Brooke BS, Habashi JP, Judge DP, Patel N, Loeys B, Dietz HC 3rd. Angiotensin II blockade and aortic-root dilation in Marfan's syndrome. N Engl J Med. Jun 26.2008 358:2787. [PubMed: 18579813]
38. Hoch JR, Stark VK, Turnipseed WD. The temporal relationship between the development of vein graft intimal hyperplasia and growth factor gene expression. J Vasc Surg. Jul.1995 22:51. [PubMed: 7602713]
39. Arking DE, Junttila MJ, Goyette P, Huertas-Vazquez A, Eijgelsheim M, Blom MT, Newton-Cheh C, Reinier K, Teodorescu C, Uy-Evanado A, Carter-Monroe N, Kaikkonen KS, Kortelainen ML, Boucher G, Lagace C, Moes A, Zhao X, Kolodgie F, Rivadeneira F, Hofman A, Witteman JC, Uitterlinden AG, Marsman RF, Pazoki R, Bardai A, Koster RW, Dehghan A, Hwang SJ, Bhatnagar P, Post W, Hilton G, Prineas RJ, Li M, Kottgen A, Ehret G, Boerwinkle E, Coresh J, Kao WH, Psaty BM, Tomaselli GF, Sotoodehnia N, Siscovick DS, Burke GL, Marban E, Spooner PM, Cupples LA, Jui J, Gunson K, Kesaniemi YA, Wilde AA, Tardif JC, O'Donnell CJ, Bezzina CR, Virmani R, Stricker BH, Tan HL, Albert CM, Chakravarti A, Rioux JD, Huikuri HV, Chugh SS. Identification of a sudden cardiac death susceptibility locus at 2q24.2 through genome-wide association in European ancestry individuals. PLoS genetics. Jun.2011 7:e1002158. [PubMed: 21738491]
40. Liu Y, Festing MH, Hester M, Thompson JC, Weinstein M. Generation of novel conditional and hypomorphic alleles of the Smad2 gene. Genesis. Oct.2004 40:118. [PubMed: 15452874]

One-sentence summary: *In vivo* endothelial cell fate mapping demonstrates that TGF-β signaling is a central pathway regulating the endothelial to mesenchymal transition (EndMT) during vein graft remodeling.

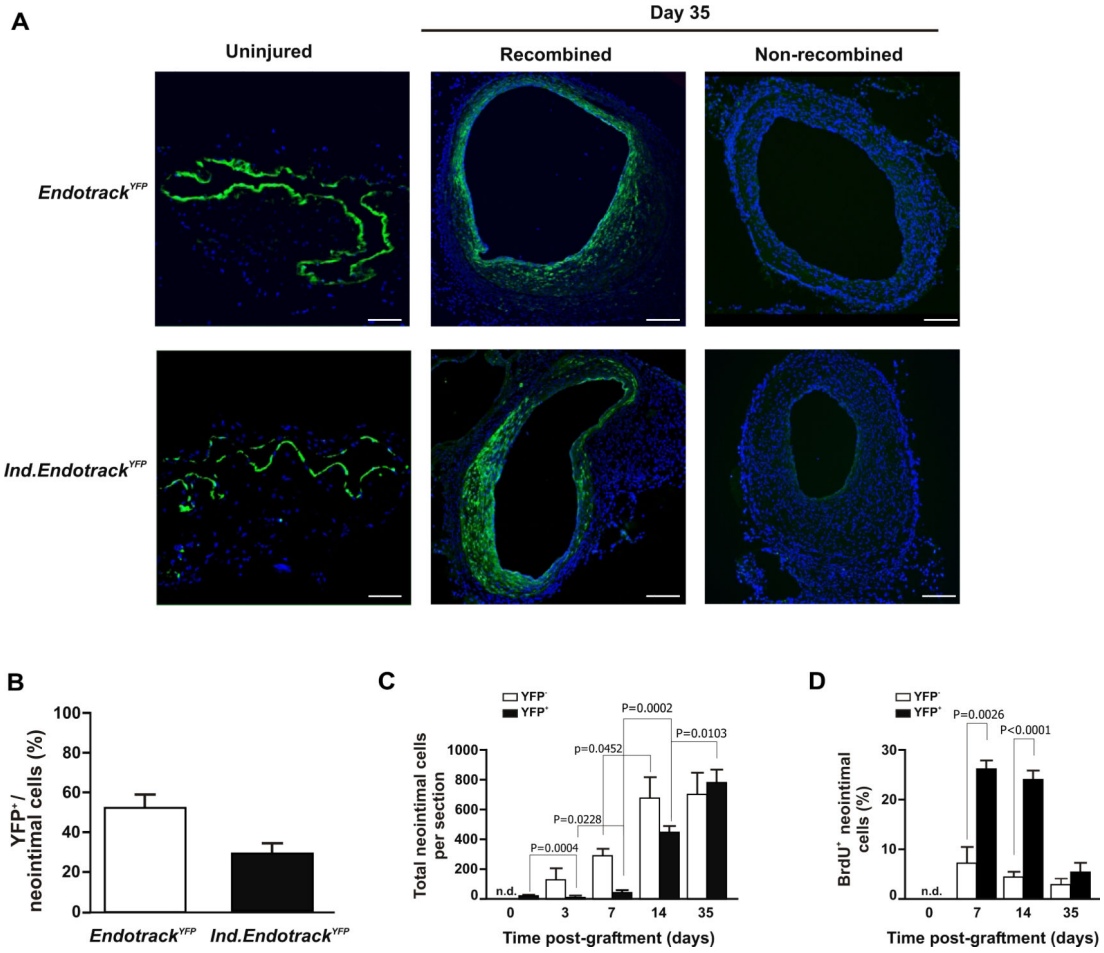

Fig. 1. Endothelial cell lineage tracing during vein graft remodeling

(A) Endothelial YFP expression in ungrafted (uninjured) jugular veins from *Endotrack*^{YFP} and *Ind.Endotrack*^{YFP} mice as well as in grafted veins from recombined and non-recombined *Endotrack*^{YFP} and *Ind.Endotrack*^{YFP} mice grafted into wild type recipients at 35 days. Scale bars, 30 μm (uninjured) and 100 μm. **(B)** The number of YFP+ cells per neointimal cells was quantified. Data are means ± SEM (n=5). **(C)** Endothelial-derived (YFP^+) and non–endothelial-derived (YFP^-) cells in the neointima over time after engraftment. Data are means ± SEM (n=4). **(D)** $BrdU^+$ cells relative to the total number of neointimal cells over time after engraftment. Data are means ± SEM (n=4). P-values in (B to D) determined by Student's *t* test.

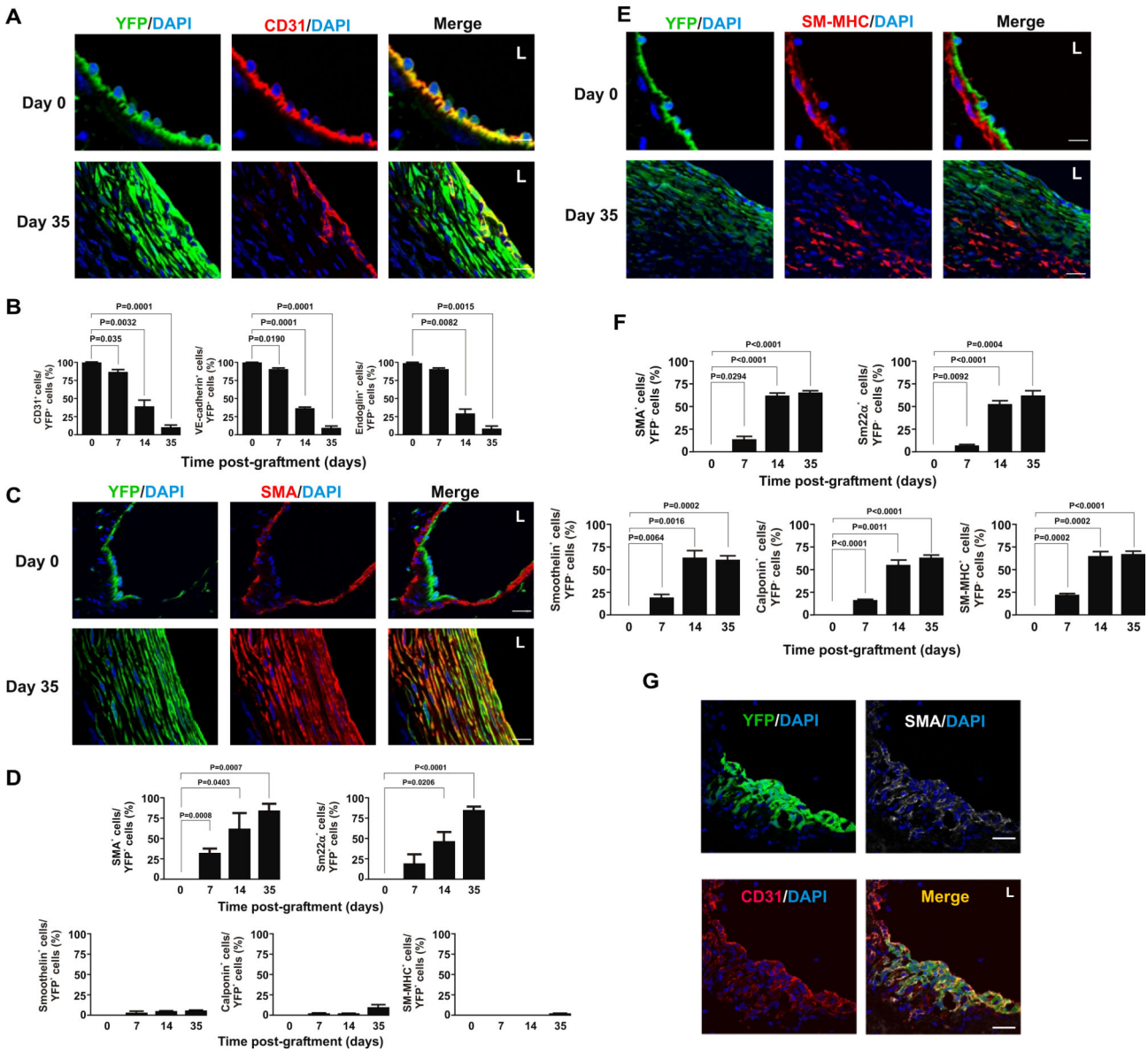

Fig. 2. EndMT during vein graft remodeling

Endotrack^{YFP} veins were grafted into wild type recipients (n = 5) and analyzed over the course of 35 days. **(A)** Immunofluorescence staining of the endothelial marker CD31 in grafted veins. **(B)** The proportion of YFP$^+$ cells expressing CD31, VE-cadherin, and endoglin over time. **(C)** SMA expression by YFP$^+$ cells. **(D)** The percentage of YFP$^+$ cells expressing immature VSMC markers SMA and SM22α and mature VSMC markers smoothelin, calponin, and SM-MHC. **(E)** SM-MHC expression in non– endothelial-derived (YFP$^-$) neointimal cells. **(F)** The percentage of non–endothelial-derived (YFP$^-$) neointimal cells expressing both immature and mature VSMC markers. **(G)** Expression of CD31 and SMA in endothelial lineage–derived (YFP$^+$) cells 7 days after grafting. Scale bars in (A, C, E, and G), 10 μm. L, lumen. Data in (B, D, and F) are means ± SEM (n=5). P-values determined by Student's *t* test. **P*< 0.05, ***P*<0.01, ****P* < 0.001

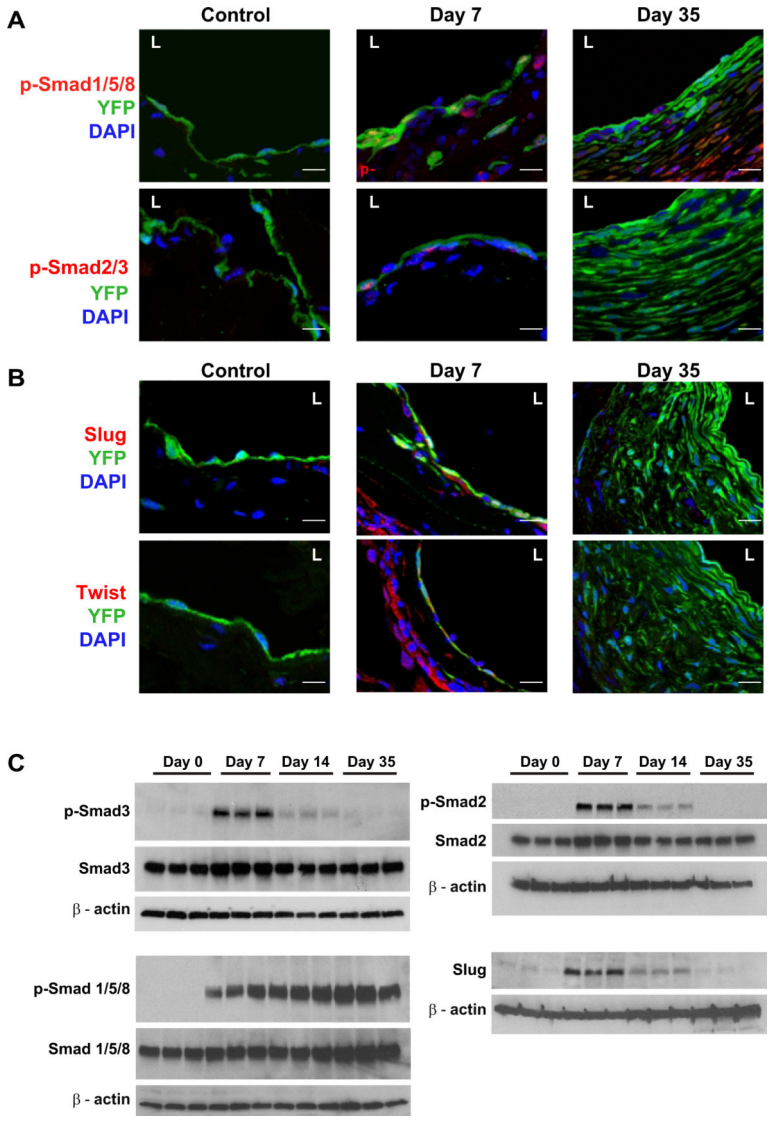

Fig. 3. TGF-β signaling during EndMT *in vivo*

Endotrack^{YFP} veins were grafted into wild type recipients (n = 3). **(A)** Immunofluorescence staining of phosphorylated Smad1/5/8 and Smad2/3 after grafting in both endothelial-derived (YFP^+) and non–endothelial-derived (YFP^-) neointimal cells. Scale bars, 5 μm. L, lumen. **(B)** Immunostaining of the TGF-β–regulated transcription factors Slug and Twist in endothelial-derived cells after grafting. Scale bars, 10 μm. L, lumen. **(C)** Western blot analysis of p-Smad3, p-Smad2, p-Smad1/5/8, and Slug from day 0 to 35 after grafting. β-actin served as loading control.

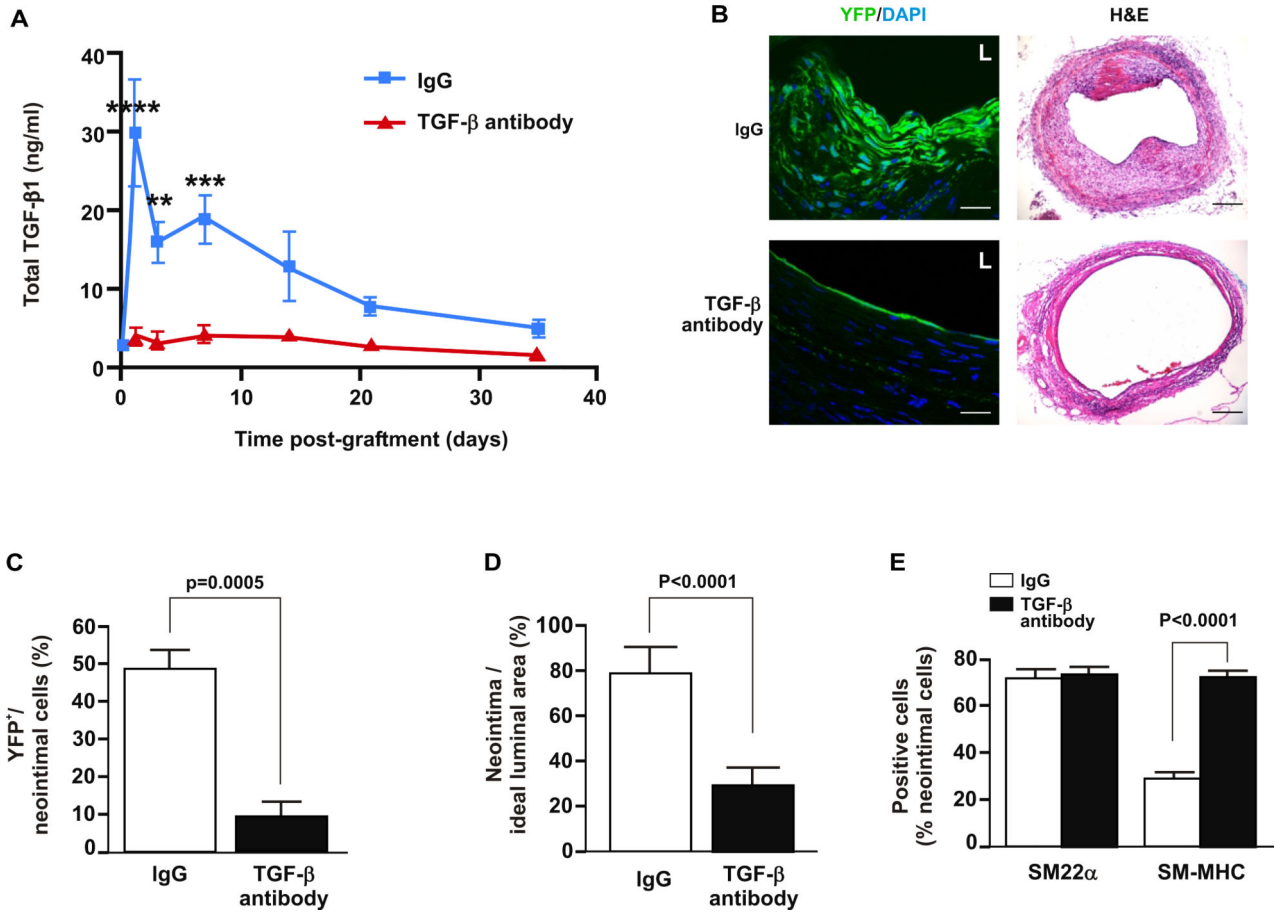

Fig. 4. A TGF-β neutralizing antibody reduces TGF-β signaling and EndMT *in vivo*

Endotrack^{YFP} veins were immersed in TGF-β neutralizing antibody or control IgG for 4 hours prior to grafting. TGF-β signaling was blocked in recipient wild-type animals by treatment with a pan–TGF-β neutralizing antibody prior to grafting, and every 14 days thereafter (n = 5 grafts per group). **(A)** Plasma levels of TGF-β1 after vein graft. Data are means ± SEM (n=5). **P<0.01, ***P < 0.001, ****P < 0.0001 ANOVA with Newman-Keuls Multiple Comparison test. **(B)** YFP expression and corresponding H&E histology of vein grafts from treated mice at day 35. Scale bars, 15 μm in YFP images, 100 μm in H&E images. L, lumen. **(C)** Percentage of endothelial-derived (YPF$^+$) cells in neointima of vein grafts treated with control or TGF-β neutralizing antibody. **(D)** Quantification of neointimal area in treated vein grafts harvested at day 35 after grafting. **(E)** The percentage of SM22α$^+$ and SM-MHC$^+$ cells in the neointima at day 35. Data are means ± SEM (n=5). P-values in (C to E) determined by Student's t test.

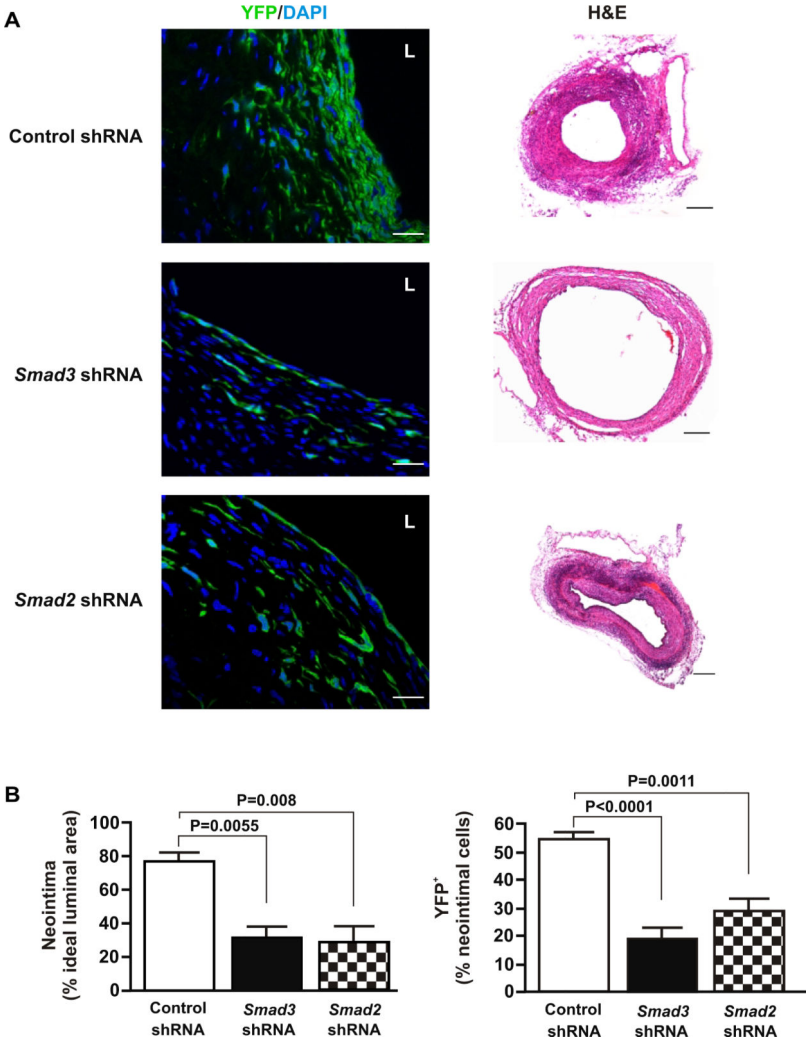

Fig. 5. Knockdown of *Smad3* or *Smad2* attenuates EndMT in mouse vein grafts

Endotrack^{YFP} veins transduced with *Smad3* or *Smad2* shRNA were grafted into wild type recipients (n = 5). **(A)** Immunofluorescence staining and H&E histology of the vein grafts harvested at day 35. Scale bars, 10 μm in YFP images, 100 μm in H&E images. L, lumen. **(B)** Quantification of the neointimal area and endothelial-derived (YFP$^+$) cells after knockdown of *Smad3* or *Smad2*. Data are means ± SEM (n = 5). P values determined by Student's *t* test.

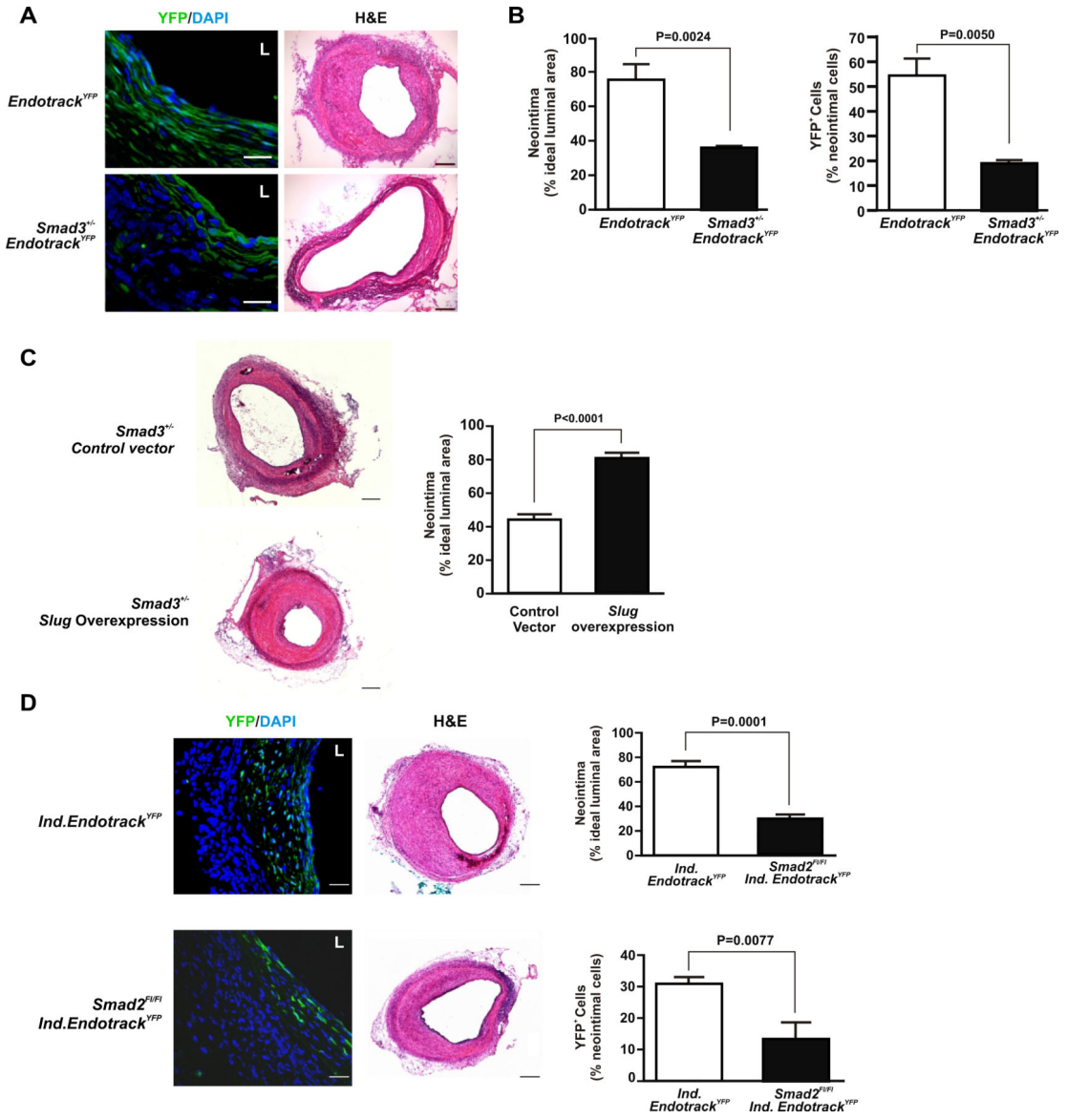

Fig. 6. Neointimal formation and EndMT in vein grafts is regulated via *Smad3* and *Slug*signaling

All data were obtained at day 35 post-grafting. **(A)** YFP and H&E staining of *Smad3*$^{+/-}$ *Endotrack*^{YFP} veins grafted into wild type recipients. Scale bars, 10 μm for YFP images; 100 μm for H&E images. L, lumen. **(B)** Quantification of neointima area and endothelial-derived (YFP^{+}) cells in the neointima. **(C)** H&E staining and quantification of neointima in *Smad3*$^{+/-}$ mouse veins overexpressing *Slug* that had been grafted into wild type recipients (*n* = 5). **(D)** Vein grafts from *Ind.Endotrack*^{YFP} and *Smad2*$^{Fl/Fl;}$*Ind.Endotrack*^{YFP} mice that had been transplanted into wild type recipients (*n* = 5) were stained for YFP or H&E. Scale bars, 15 μm for YFP images L, lumen; 100 μm for H&E images. Quantification of YFP^{+} endothelial-derived cells and neointimal area. Data in (B to D) are means ± SEM (*n* = 5). P-values determined by Student's *t* test.

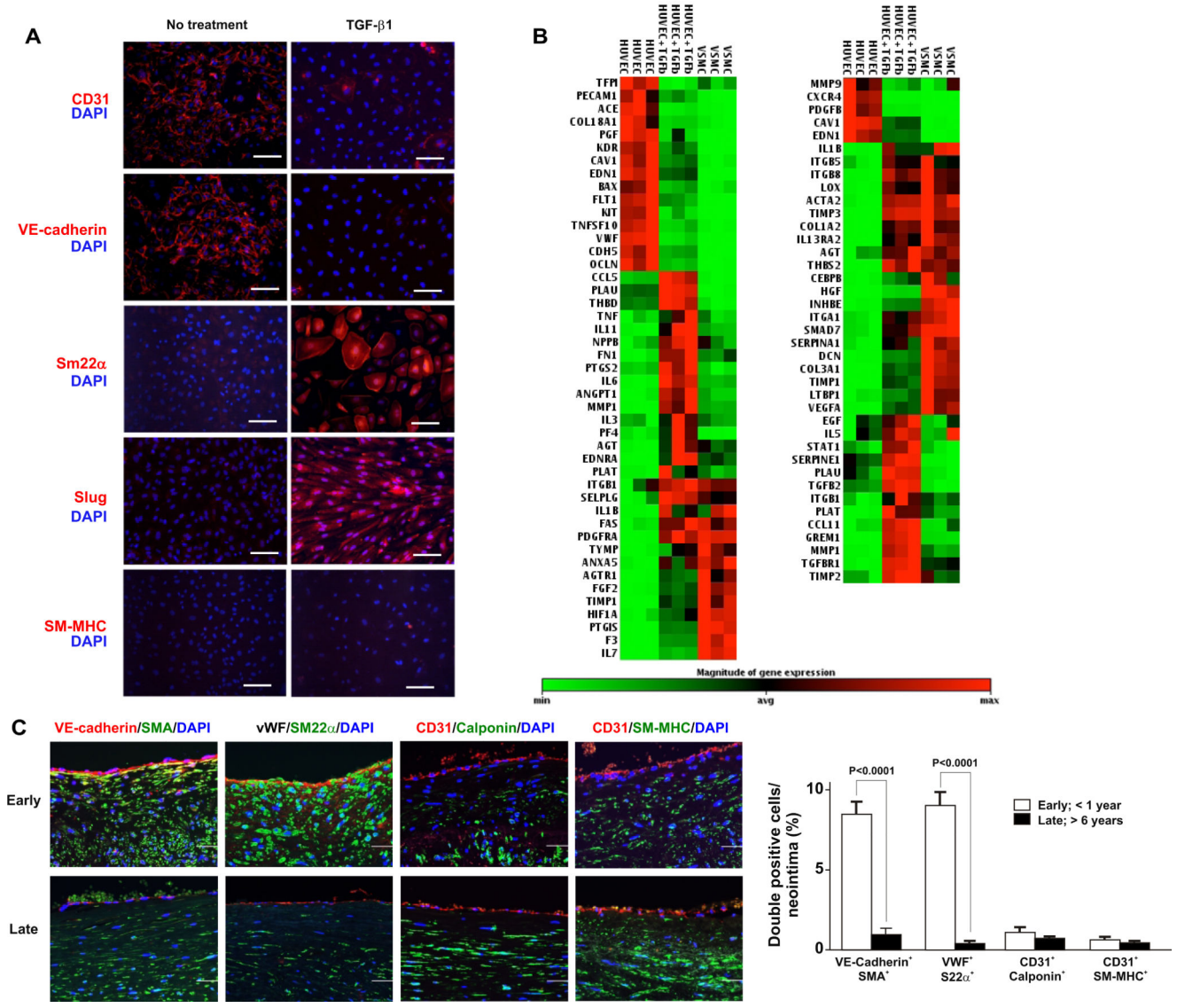

Fig. 7. EndMT in human endothelial cells and in human vein graft remodeling

(A) HUVECs were treated with 10 ng/ml TGF-β1 and stained for CD31, VE-cadherin, SM22α, Slug, and SM-MHC. Scale bars, 10 μm. Images are representative of n=3 experiments. **(B)** Human RT2 PCR Arrays were used to assess gene expression in baseline HUVECs ± TGF-β1 and human aortic VSMCs. Data represent significant ($P \leq 0.05$, Student's *t* test) 2-fold differentially regulated gene expression in HUVECs compared to HUVECs with TGF-β1. **(C)** EndMT observed in tissue samples after during human vein graft remodeling. Immunofluorescence co-staining of early (<1 year, n=5) and late (>6 year, n=5) human vein grafts with endothelial (VE-cadherin, vWF) and immature (SMA, SM22α) or mature (SM-MHC, calponin) VSMC markers. Scale bars, 100 μm. Graph depicts quantification of EndMT (double-positive staining) in human vein grafts (n=5 per group). P-values determined by Student's *t* test.